

Technical manual No.G006-E

Faraday Rotator ( **R**are-earth **I**ron **G**arnet single crystals )

**GRANOPT**

6/1/2015

## CONTENTS

1. Type of Faraday Rotators	2	7. Anti-Reflection Coating (AR Coating)	19
2. Order Information		7-1. AR coating types	
3. Properties		7-2. Features	
4. Rare-Earth Iron Garnet Single Crystal	3	7-2-1. Coating ( A ) for air	
4-1. Crystal structure		7-2-2. Coating ( E ) for epoxy	20
4-2. Optical properties	4	7-3. Incident angle	
4-3. Magnetic properties	5	8. Reliability Test	
4-4. Lead impurities		8-1. Environment test	
5. Optical Properties	6	8-2. Laser damage	21
5-1. Faraday rotation angle and extinction ratio		8-2-1. Laser damage by plus laser	
5-1-1. Measurement method		8-2-2. Temperature rise by light absorption	
5-1-2. Wavelength dependence		9. Surface Quality	22
5-1-3. Temperature dependence	7	9-1. Standard specifications	
5-1-4. Effect of incident angle	8	9-2. Influence of defect and AR pinhole	
5-1-5. Effect of stress	9	9-3. RIG scratch and AR scratch	23
5-2. Insertion Loss and refractive angle	10	9-4. Chipping and corner break	
5-2-1. Measurement equipment		10. Appendixes	24
5-2-2. Insertion loss		10-1. Growth Striation	
5-2-3. Refractive angle and coupling loss	11	10-2. Swirl	
5-2-4. Temperature dependence		10-3. Surface Undulation	
5-3. External field and optical properties	12		
5-3-1. Faraday angle and extinction ratio			
5-3-2. Diffraction phenomena by magnetic domain	13		
6. Magnetic Properties	14		
6-1. Magnetization curve			
6-2. Saturation field			
6-3. Coercive force	15		
6-3-1 Magnet-free Faraday Rotator	16		
6-3-2 How to use GMF	17		
6-4. Magnetic Compensation temperature and Curie temperature	18		

## 1. Type of Faraday Rotators

This technical document describes the properties of Faraday rotators of GRANPT. All Faraday rotators of GRANOPT comply with RoHS (Restriction of the use of the certain Hazardous Substances).

### G-series

**GTD** ( **TD** represents **T**emperature **D**ependence )

Features small temperature dependence and small wavelength coefficient. This product is generally used for free space optical isolators.

**GLB** ( **LB** represents **L**-**B**and )

Features small insertion loss in the L-band wavelength and is generally used for in-line optical isolators.

**GSF** ( **SF** represents **S**aturation **F**ield )

Features lower saturation field. This Faraday rotator is used to reduce the size of an optical isolator or used for a magneto-optical switch that changes the direction of Faraday rotation in a magnetic field.

**GMF** ( **MF** represents **M**agnet-**F**ree )

Dose not need an external magnetic field from permanent magnetic etc.

### E-series

**ETD** ( **TD** represent **T**emperature **D**ependence )

Has the same characteristics as the GTD but contents no lead.

## 2. Order Information

When you place an order, specify the product as described below.

AAABBBBCD – Other information	ex. <u>GTD</u> <u>1550</u> <u>L</u> <u>A</u>
AAA Garnet	GTD, GLB, GSF, GMF, ETD
BBBB Wavelength	1550(nm); 1310(nm), etc.
C Size	L; 11mm square C; Chip Size
D AR-coating	A; For air E; For epoxy N; non coating X; else
– Other information	ex. Accuracy of rotation angle, chip size, etc.
	* If your demand is different from the standard specifications, contact us.

Wavelength coefficient,  $\Delta\theta/\Delta\lambda$ (deg/nm) for 45deg-rotator

	GTD	GLB	GSF	GMF	ETD
1310nm	0.085	/	0.085	0.085	0.085
1480nm	0.07	0.075	0.075	0.075	0.07
1550nm	0.06	0.07	0.065	0.065	0.06
1590nm	0.055	0.065	0.06	0.06	0.055

Temperature coefficient,  $\Delta\theta/\Delta T$  (deg/C) for 45deg-rotator

	GTD	GLB	GSF	GMF	ETD
1310nm	0.04	/	0.07	0.07	0.04
1480 - 1590nm	0.045	0.065			0.045

Insertion loss(dB)

	GTD	GLB	GSF	GMF	ETD
1310 - 1550nm	0.1	0.05	0.1	0.1	0.1
1590nm	0.16		0.12	0.16	0.16

Thickness( $\mu$ m) (typical)

	GTD	GLB	GSF	GMF	ETD
1310nm	310	/	320	280	310
1550nm	450	390	475	420	450

Magnetic property

	GTD	GLB	GSF	GMF	ETD
Hs(Oe)	700	800	200	/	700
Tcomp.(C)	<-50	<-50	-50	0	<-50
Tc(C)	300	300	250	230	300
Hc(Oe)	/	/	/	500	/

Hs ; Saturation field for 1mm square chip. See Section 6-2.

Tcomp. ; Magnetic compensation temperature

Tc ; Curie temperature

Hc ; Coercive force

## 3. Properties

#### 4. Rare-Earth Iron Garnet Single Crystal (RIG) 4-1. Crystal structure

GRANOPT manufactures bismuth-substituted rare-earth iron garnet (RIG) single crystals which are material for Faraday rotator using the liquid phase epitaxial (LPE) method.

RIG, a very stable oxide with the chemical formula  $(C_3)(A_2D_3)O_{12}$  is a single crystal having the structure of a cubic system as shown Fig. 4-1. Table 4-1 and Fig.4-2 show the physical properties of RIG.

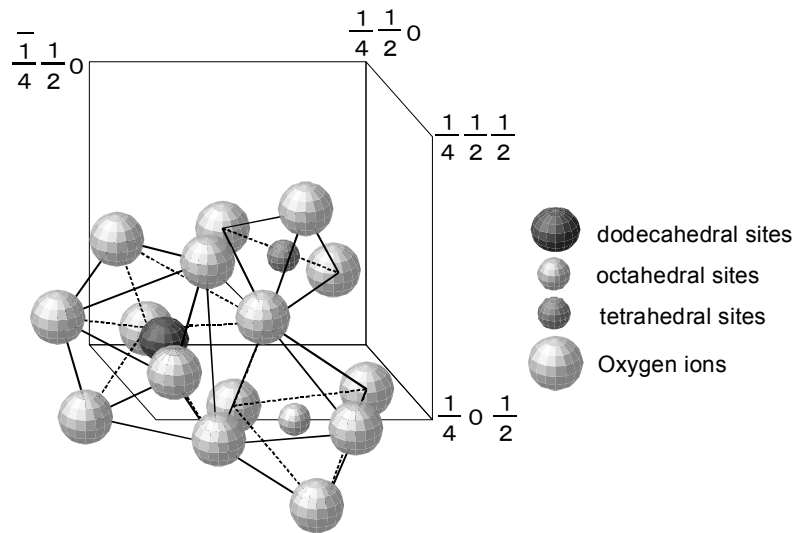


Fig.4-1 Crystal structure

Table. 4-1 Physical properties

	GTD	GLB	GSF	GMF	ETD
Lattice parameter (Å)	12.5				
Thermal expansion coefficient ( $10^{-6} K^{-1}$ )	11		10		11
Refractive index (1550nm) * Fig.4-2	2.3 – 2.4				
Mohs' scale*	7				
Young's modulus*(GPa)	200				
Poisson's ratio*	0.29				
Density*(g/cm <sup>3</sup> )	6.7				
Thermal conductivity*(W/m K)	5				
Heat capacity*(J/mole K)	420				

\* Estimation based on references.

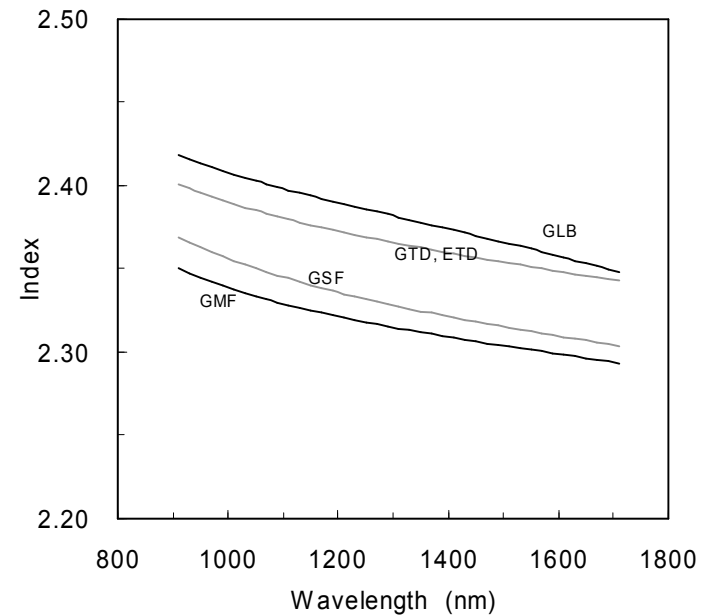


Fig.4-2 Refractive index of Faraday rotator.

## 4-2. Optical properties

RIG is a magneto-optical material that is transparent in the near infrared radiation region and mid-infrared radiation region with a wavelength of 1 to 5 $\mu\text{m}$  and has a very large Faraday effect. The Faraday effect is a phenomenon in which the polarization plane of the light is rotated when the light passes through a magnetized material. This rotation is caused by differences in response between the left and right circular polarization.

RIG has very large Faraday rotation coefficient of 1000 to 2000 (deg/cm) in the near-infrared radiation region. Fig. 4-3 shows the Faraday rotation coefficient of the GTD, that is, the Faraday rotation angle per centimeter. The magnitude, wavelength dependence, and temperature dependence of the Faraday rotation coefficient vary with the product. Refer to Chapter 3 for details. In our products, the film thickness is adjusted so that the Faraday rotation angle becomes 45 degrees at a specified wavelength.

Letting linearly polarized light pass through RIG causes Faraday rotation, but the ellipticity of the linearly polarized light increases more or less. This ellipticity is expressed by extinction ratio. The extinction ratio is affected by magneto-optics, external stress of the material (see Section 5-1-4), the performance of AR coating (see Section 5-1-4), etc. In addition, if the property (mono-chromaticity) of a light source used for measurement is low, the extinction ratio may become low due to the wavelength dependence of the Faraday rotation angle shown in Fig. 4-3.

Because all types of RIG contain iron ions that have optical absorption, the RIG is not opaque in the visible range. Some of our products other than the GLB may have high insertion loss in the L band due to weak optical absorption by rare earth ions. Refer to Section 5-2 for details.

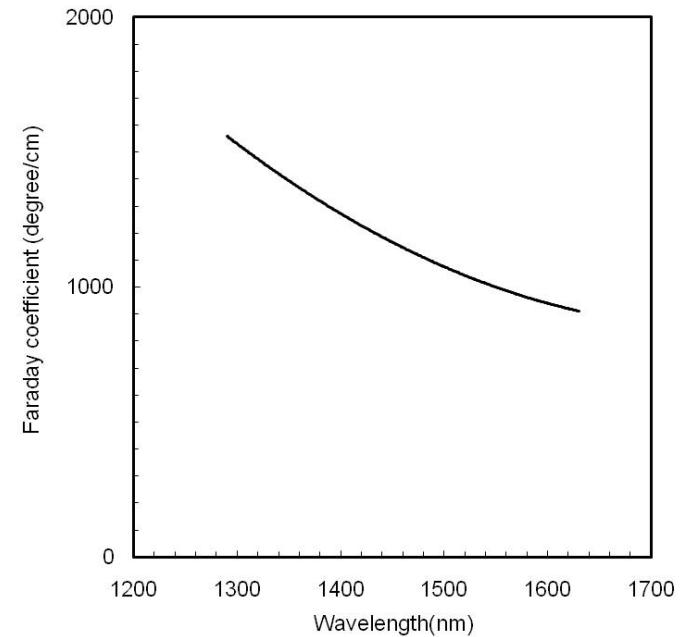


Fig.4-3 Wavelength dependence of Faraday coefficient

### 4-3. Magnetic properties

RIG is a ferrimagnetic material, which is one of ferromagnetic materials. Generally, a ferromagnetic material has a magnetic domain where magnetization is aligned in the same direction. The RIG manufactured by the LPE method of GRANOPT has a maze-like domain structure in which two magnetic domains are oriented in two mutually opposite directions orthogonal to the film surface as shown in Photo 4-1. Because the light beams that pass through these two magnetic domains rotate in mutually opposite directions, the extinction ratios of the light beams are degraded, causing interference of the transmitted light beams (refer to Section 5-3). Therefore, it is not possible to use the RIG as a Faraday rotator without applying a magnetic field.

When RIG is exposed to an external magnetic field greater than its saturation field, the magnetic domain in the direction opposite to the external magnetic field disappears and a single magnetic domain in which the direction of magnetization is aligned is formed. Since light passing through RIG with a single magnetic domain is subject to Faraday rotation in one direction, the RIG can be used as a Faraday rotator.

Once magnetized in a strong external magnetic field, the GMF retains its single domain structure even if the external magnetic field is removed. Thus, the GMF requires no external magnetic field when it is used. In other words, the GMF functions as a Faraday rotator without being exposed to an external field. Refer to Chapter 6 for details.

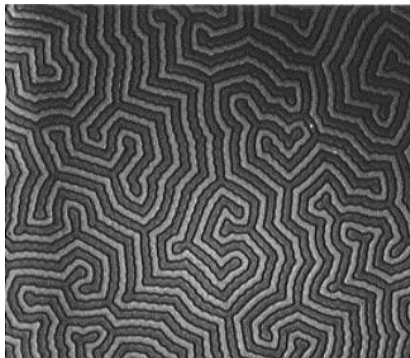


Photo 4-1 Domain structure of RIG

### 4-4. Lead impurities

GRANOPT manufactures RIG from a flux including lead dioxide using a crystal growth method called LPE method. Our RIG products conventionally included about 5,000ppm lead as impurities. We have developed the technology to control the lead content in RIG and provided the G-series Faraday rotators, including the GTD, GLB, GSF, and GMF. In addition, we have developed lead free RIG, the ETD Faraday rotator. Fig. 4-4 shows the distribution of lead content of the G-series products. The lead content is controlled to less than 1,000ppm so that all the products comply with RoHS.

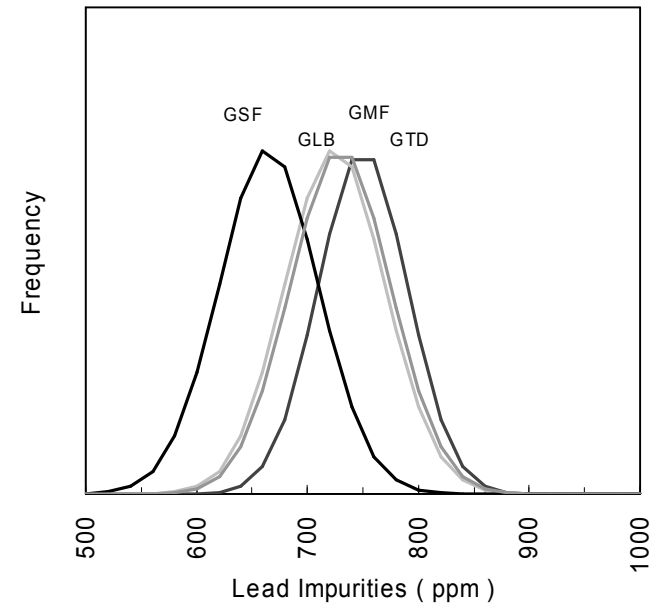


Fig.4-4 Lead impurities

## 5. Optical Properties

### 5-1. Faraday rotation angle and extinction ratio

#### 5-1-1. Measurement method

Fig. 5-1 shows the basic structure of the measurement equipment used to measure the Faraday rotation angle and extinction ratio. A DBF laser with a high mono-chromaticity is used as the light source. The rotation angle and extinction ratio are measured using a personal computer that controls a polarizer, analyzer, sample holder, detector, and thermometer.

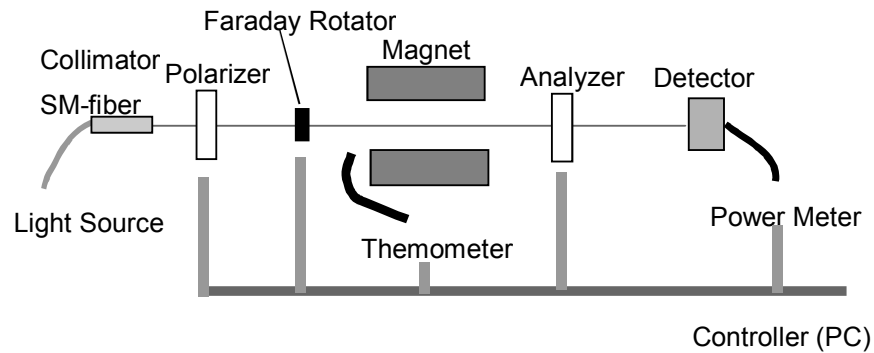


Fig.5-1 Measurement equipment for Faraday angle and extinction ratio

#### 5-1-2. Wavelength dependence

Figs. 5-2 and 5-3 show changes in the Faraday rotation angle of the GTD with respect to the wavelength. The tables in Chapter 3 list the wavelength dependence of typical Faraday rotation angles for the individual products. In the wavelength dependency, changes in the Faraday rotation angle per 1-nm for 45-degree Faraday rotators. There no significant differences are present in the O-band and E-band, but large differences are present in the C-band and L-band.

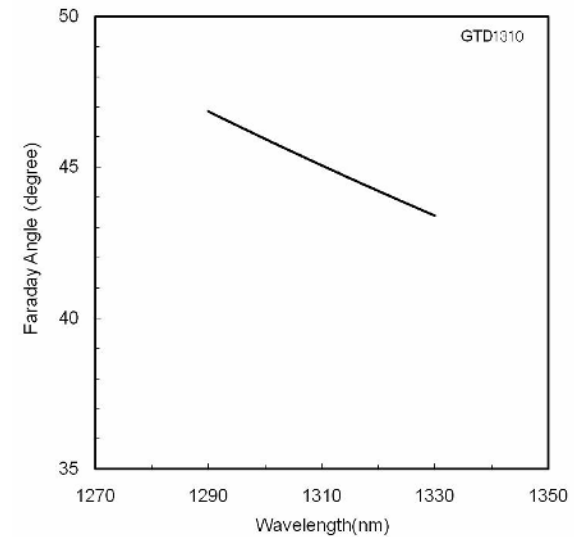


Fig.5-2 Wavelength dependence

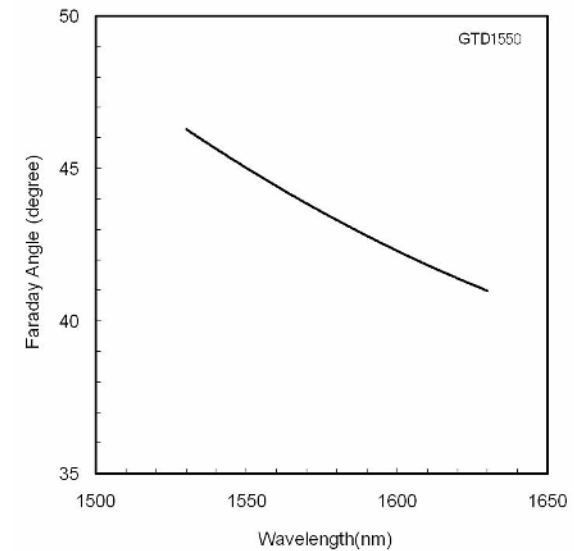


Fig.5-3 Wavelength dependence

### 5-1-3. Temperature dependence

Fig. 5-4 and 5-5 show changes in the Faraday rotation angle of the GTD with respect to the temperature. We define the changes in the rotation angle of a 45 degree Faraday rotator per one degree as the temperature dependence by using the value calculated from the data measured in the range of 0°C to 50°C. The temperature dependence of the GTD and ETD slightly differs between 1310nm and 1550nm. In other products, the rotation angle depends on the model, but does not greatly depend on the wavelength.

From Fig. 5-6, it is found that the extinction ratio do not depend on the temperature.

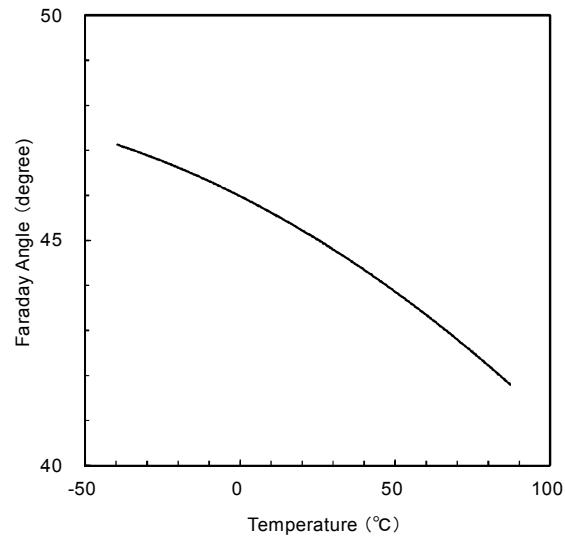


Fig.5-4 Temperature dependence of Faraday angle

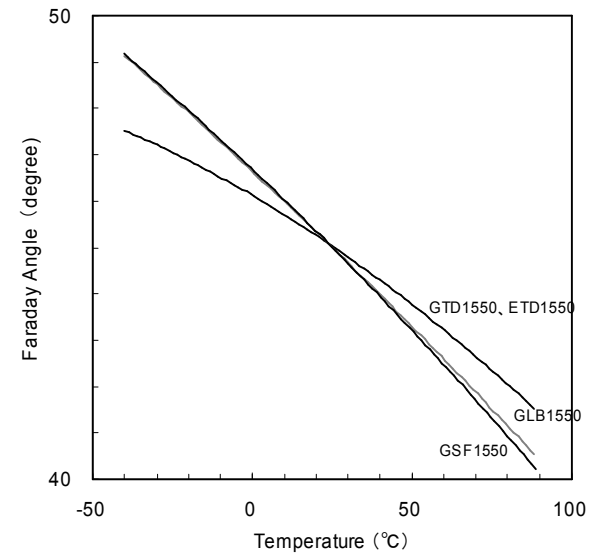


Fig.5-5 Temperature dependence of Faraday rotation angle

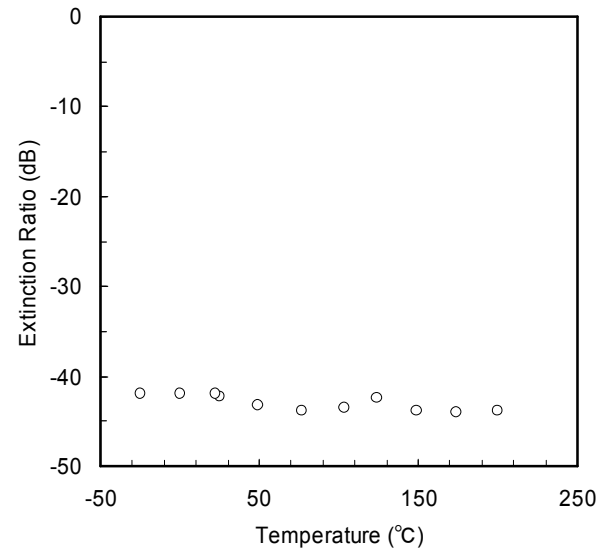


Fig.5-6 Temperature dependence of extinction ratio

### 5-1-4. Effect of an Incident Angle

Filled circles in Fig. 5-8 show an example of measuring the Faraday rotation angle by changing the incident angle of light with respect to the Faraday rotator. Open circles show an example of measuring the extinction ratio in the same condition.

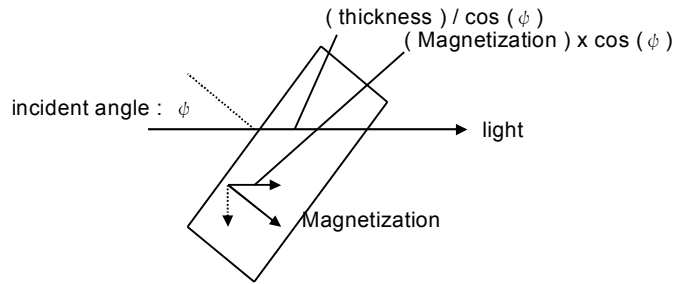


Fig. 5-7 Incident angle and magnetization

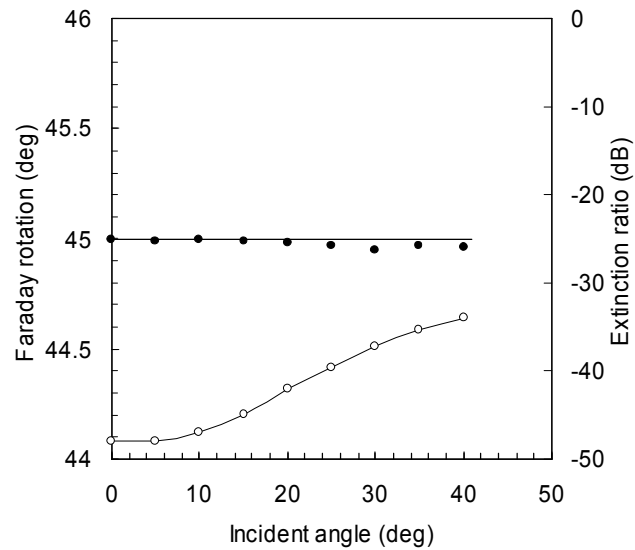


Fig. 5-8 Measurement of Faraday rotation angle and extinction ratio

The reason why the Faraday rotation angle does not depend on the incidence angle of light will be described with reference to Fig. 5-7. The direction of magnetization has an effect on the Faraday rotation angle. General RIG is magnetized perpendicularly to the film surface because of its magnetic anisotropy. The length of the path of light passing through RIG becomes longer even when the light enters at the slant, but the effect of magnetization is reduced. Therefore, certain Faraday rotation is applied.

On the other hand, the extinction ratio reduces as the incident angle increase. This is because the performance of the AR coating is degraded. Degradation in the performance of AR coating causes part of light to make multiple reflections in the RIG. The multiple reflection light that transmits in the same direction as in the incident light receives the Faraday effect three to five times more than the normal one and the multiple reflection light affects the measurement result of the extinction ratio.

From Fig. 5-9, which shows the relationship between the incident light and the insertion loss, it is found that generation of the multiple reflection light causes reflection and increases insertion loss.

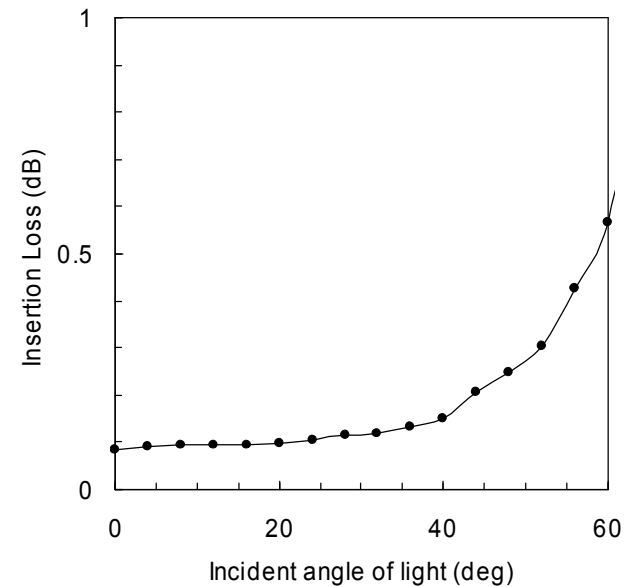


Fig. 5-9 Measurement of insertion loss

### 5-1-5. Effect of stress

The extinction ratio is also degraded by a stress. Fig. 5-11 shows the measurement result of the extinction ratio by applying an external stress to the Faraday rotator as shown in Fig. 5-10. Degradation in the extinction ratio is caused by photoelasticity. The horizontal axis in Fig. 5-11 represents the angle formed by the polarization direction of incident light and the direction of stress. When this angle is 22.5 degrees, the extinction ratio or the effect becomes minimum. This is because the polarization plane of the incident light rotates orthogonal to the stress direction by -45 degrees.

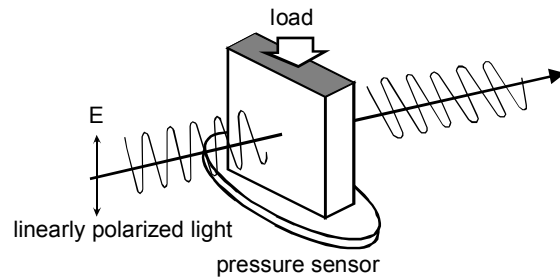


Fig. 5-10 Measurement method

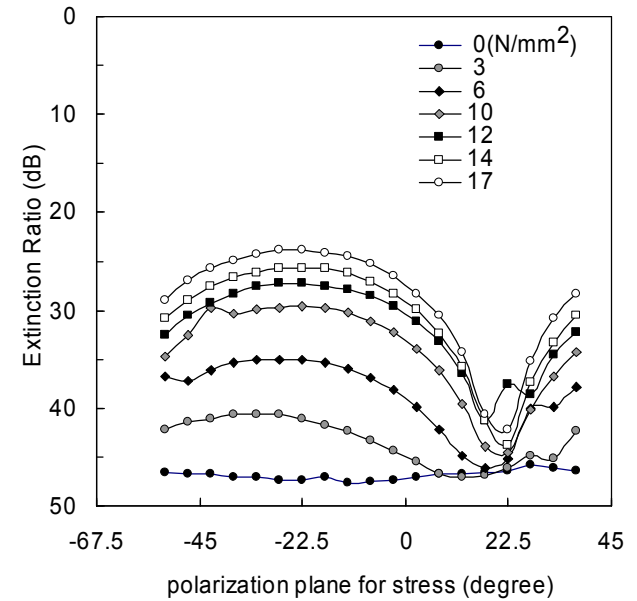


Fig. 5-11 Degradation in extinction ratio due to external stress

## 5-2. Insertion loss and refractive angle

### 5-2-1. Measurement equipment

Fig. 5-12 shows the structure of equipment for measuring the insertion loss and refractive angle. The light source is a PF laser, DFB laser, or a variable wavelength laser. A personal computer is used to control the slit for measuring the refractive angle, the sample holder, and the detector. This equipment can measure the insertion loss and refractive angle individually.

The insertion loss is defined as the difference in the strength of transmitted light between presence and absence of the sample. The refractive angle is calculated from the attenuation of light passing through the slit.

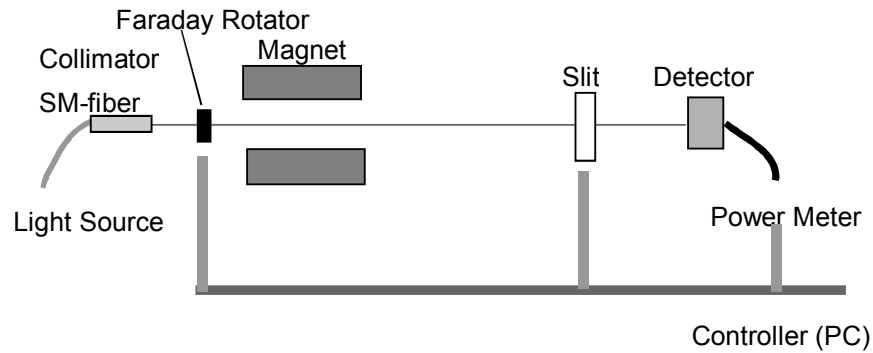


Fig.5-12 Structure of equipment for measuring insertion loss and refractive angle

### 5-2-2. Insertion loss

Fig. 5-13 shows the measurement result of insertion loss in the C- and L-bands for the individual products. In the products other than the GLB, insertion loss increases in the L-band due to weak absorption by rare earth ion. Accordingly, in the L-band, use of the GLB is recommended.

Fig. 5-14 shows the insertion loss of the GLB in the short wavelength. The products other than the GLB have an insertion loss of more than 1.5 times of this value. Accordingly, also in the short wavelength, use of the GLB is recommended.

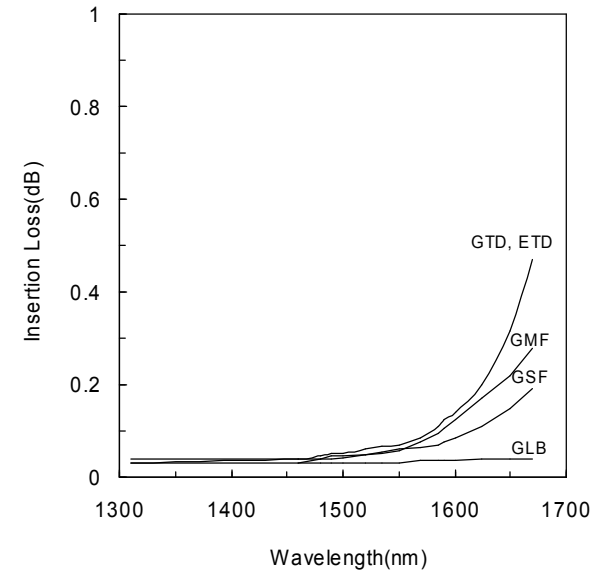


Fig.5-13 Insertion loss of individual product

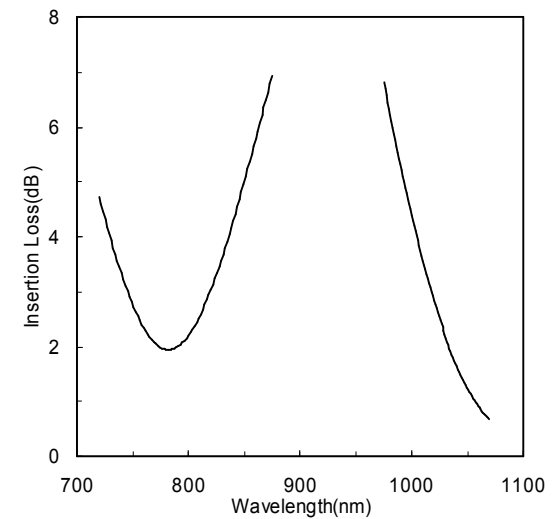


Fig.5-14 Insertion loss of GLB in short wavelength

### 5-2-3. Refractive angle and coupling loss

The insertion loss of the in-line optical isolator consists of insertion loss by optical absorption in a Faraday rotator and coupling loss by refraction of light (refractive angle) by a Faraday rotator. GRANOPT defines insertion loss separately from coupling loss by refraction of light by a Faraday rotator and determine different specifications. GRANOPT does not guarantee the coupling loss. This is because the coupling loss is indirectly affected by the refractive angle of a Faraday rotator through the structure of the collimator or other components.

### 5-2-4. Temperature dependence

Figs. 5-11 and 5-16 show the measurement result of temperature dependence of the insertion loss.

Fig. 5-15, which is the measurement result for the GTD1310, shows that insertion loss is not temperature-dependent in the wavelength band in which no absorption loss is present. However, as shown in Fig. 5-16, insertion loss is temperature-dependent in a wavelength band close to  $1\mu\text{m}$  in which absorption loss is present.

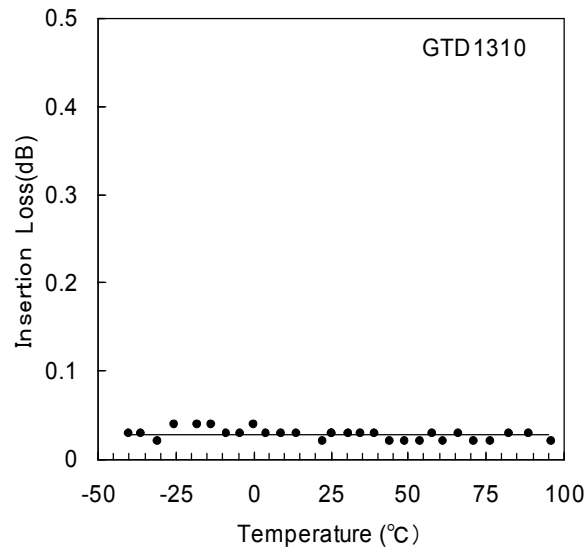


Fig. 5-15 Temperature dependence of insertion loss of GTD1310

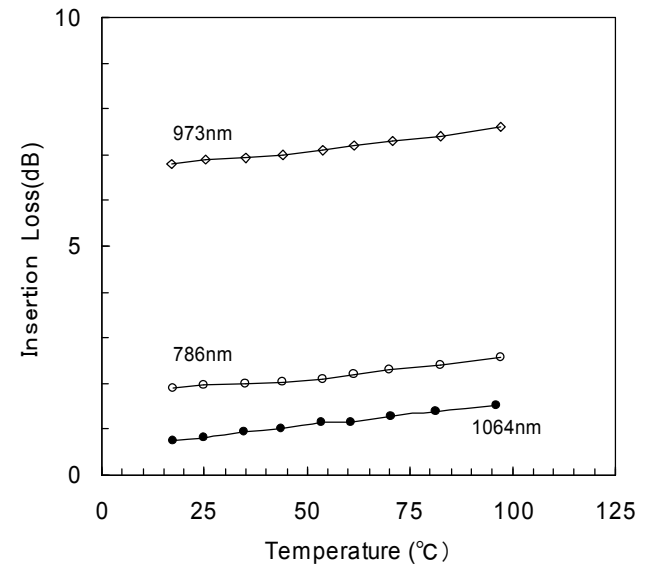


Fig. 5-16 Temperature dependence of insertion loss of GLB in short wavelength

5-3. External field and optical properties  
 5-3-1. Faraday angle and extinction ratio

When RIG is not magnetically saturated, the multi-domain structure as shown in Photo 4-1 is formed in the RIG. When light beams pass through RIG that is not magnetically saturated, the light beams passing through the individual domains are subject to Faraday rotation in the two opposite directions and diffraction is caused by the interference of the individual light beams (refer to Section 5-3-2). As a result, the light beams passing through the RIG are detected as a sum of light components that have passed and scattered in the magnetic domains.

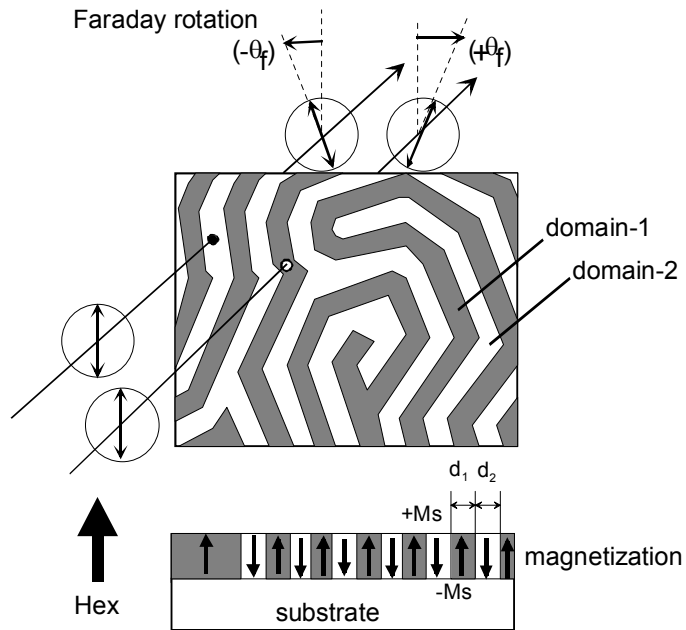


Fig. 5-17 Multi-domain structure and Faraday rotation of RIG

Fig. 5-18 shows the measurement result of the Faraday rotation angle and the extinction ratio with respect to an external magnetic field. The Faraday rotation angle apparently changes in proportion to the external magnetic field. However, it can be seen from the reduction in the extinction ratio that the Faraday rotation angle does not change linearly. The Faraday rotation of RIG is theoretically quite different from the magneto-optical effect proportional to the external magnetic field as expressed by the Verdet's constant.

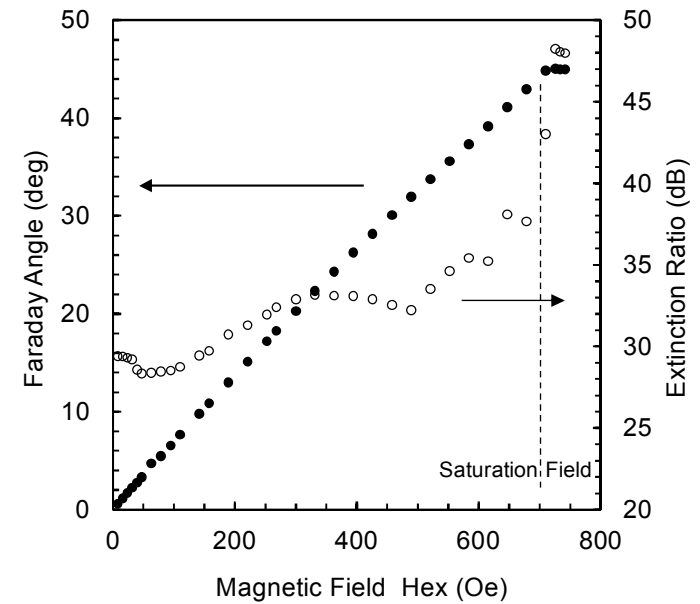


Fig. 5-18 Measurement of Faraday rotation angle and extinction ratio in multi-domain structure.

### 5-3-2. Diffraction phenomena by magnetic domain

When light passed through a magnetically unsaturated Faraday rotator, diffraction is caused by the multi-domain structure as shown in Fig. 5-19. As the Faraday rotation that depends on the difference in the area of a magnetic domains is caused in 0-dimensional transmitted light( $n=0$ ), apparently constant Faraday rotation is observed with respect to the polarization plane of incident light while the diffracted light has the polarization plane perpendicular to the polarization plane of incident light. For example, for a 45-degree Faraday rotator, the maximum amount of light diffracted is about -3dB or about -1dB as actual measurement data, which depend on the multi-domain structure. The reason why the insertion loss of a magnetically unsaturated Faraday rotator appears to be larger when using a detector with a finite size is because of this.

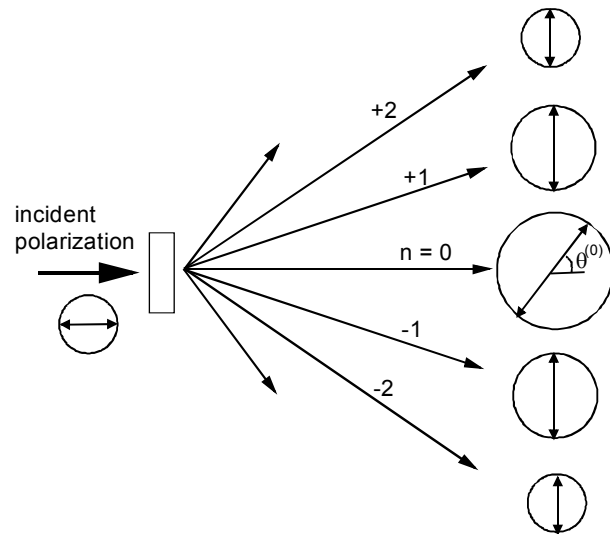


Fig. 5-19 Diffraction by multi-domain structure

## 6. Magnetic properties

### 6-1. Magnetization curve

Fig.6-1 shows the structure of equipment for measuring the magnetization curve of a Faraday rotator. When an external magnetic field is applied to a Faraday rotator, the width of magnetic domains changes according to the external magnetic field. Light transmitted through or diffracted in the magnetic domains is separated into two mutually orthogonal components by the analyzer. Then, the magnetization curve of the Faraday rotator can be drawn by taking the differences between these two components. Fig. 6-2 shows the magnetization curve of the GTD measured by this equipment.

Saturation field  $H_s$ , nucleation magnetic field  $H_n$ , and coercive force  $H_c$  can be read from this magnetization curve.

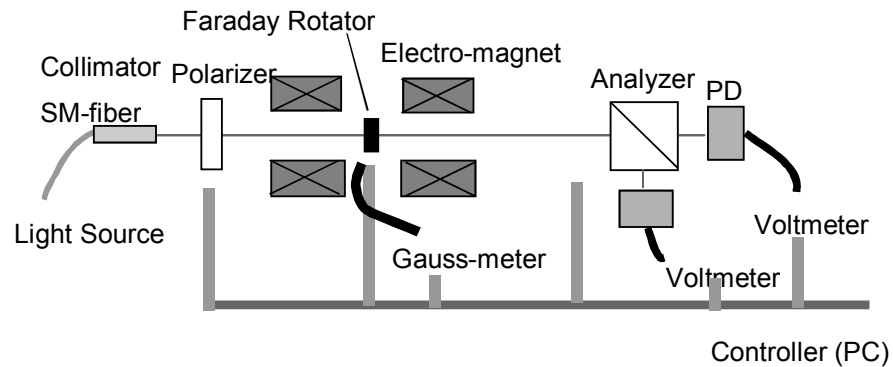


Fig. 6-1 Structure of measurement equipment for magnetization curve

Saturation field  $H_s$  :

The saturation field is the magnetic field at which a Faraday rotator becomes saturated magnetically or shifts from the multi-domain structure to the single domain structure. When a magnetic field greater than the saturation field is applied, a Faraday rotator has a fixed Faraday rotation angle. The saturated magnetic field depends on the shape of the Faraday rotator. Refer to Section 6-2 for details,

Nucleation magnetic field  $H_n$  :

When the external magnetic field required for magnetic saturation is reduced, the domain structure appears at the specific magnetic field. We define this specific magnetic field as nucleation magnetic field  $H_n$ . Refer Section 6-4 for details.

Coercive force  $H_c$  :

In the GMF, the domain structure does not appear even if the applied external magnetic field is reduced, but the direction of magnetic field is reversed when a magnetic field in the opposite direction is applied. This magnetic field at which magnetization is reversed is called a coercive force. Although coercive force  $H_c$  is almost the same as nucleation magnetic field  $H_n$  theoretically, we defines this value as coercive force  $H_c$  only for the GMF. Refer to Section 6-3 for details.

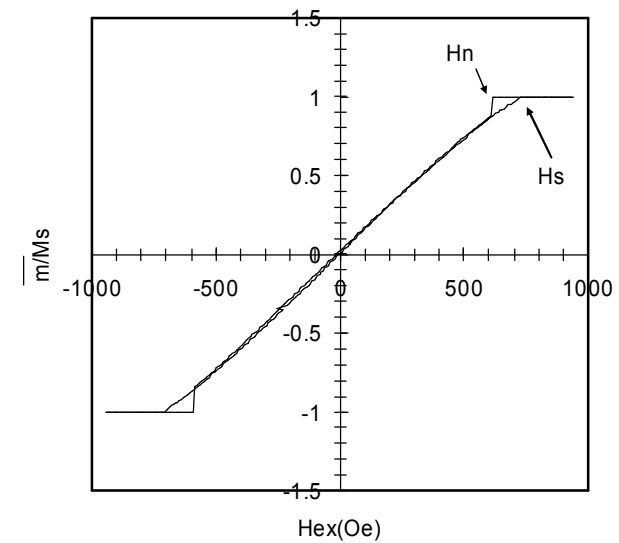


Fig. 6-2 Magnetization curve of GTD

## 6-2. Saturation field

When an external magnetic field greater than the saturation field of RIG is applied, RIG is magnetically saturated and functions as a Faraday rotator. Therefore, when a product other than the GMF is used, it is necessary to use a permanent magnet that can apply an external magnetic field value greater than saturation field  $H_s$ . Fig. 6-3 illustrates the temperature dependence of saturation field  $H_s$  of the GTD and ETD. Fig. 6-4 illustrates the temperature dependence of saturation field  $H_s$  of the GSF. Note that the saturation field depends on the temperature. We define the saturation field required in the temperature range from  $-20^{\circ}\text{C}$  to  $85^{\circ}\text{C}$  as the specification.

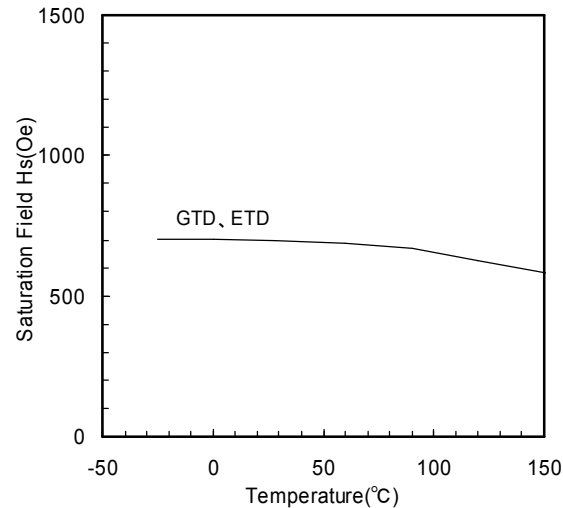


Fig. 6-3 Temperature dependence of saturation field of GTD and ETD

Saturation field  $H_s$  depends on the shape of a product. Fig. 6-5 shows the approximation of the shape of a product and the demagnetization factor. The horizontal axis represents the size-to-thickness ratio and the vertical axis represents the demagnetization factor. The saturation field for a flat plate of infinite size (the horizontal axis is  $\infty$  and the demagnetization factor is 1) multiplied by the demagnetization factor in Fig. 6-5 is the saturation field for the actual product size. A product with a smaller size and a larger thickness has a smaller demagnetization factor and smaller saturation field. We define the saturation field of a 1mm chip, which is used generally, as the specification.

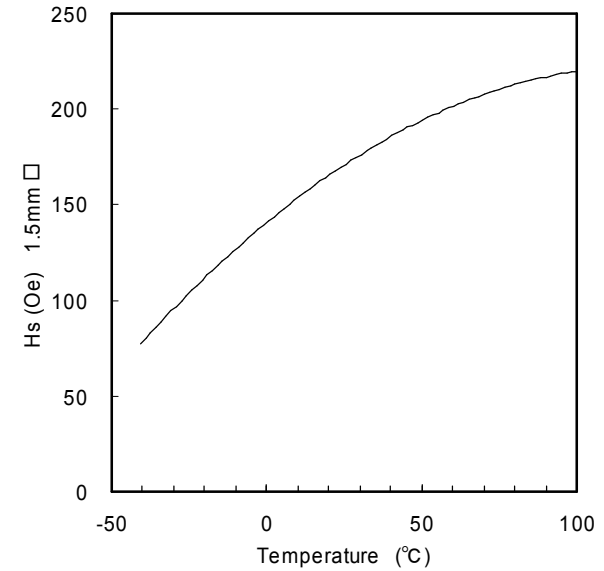


Fig. 6-4 Temperature dependence of saturation field of GSF

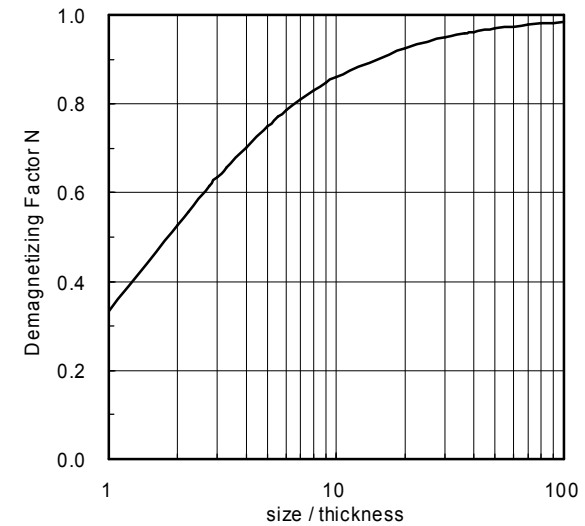


Fig. 6-5 Geometrical shape and demagnetization factor

6-3. Coercive force  
 6-3-1. Magnet-free Faraday rotator

Fig. 6-6 illustrates the magnetization curve of the magnet-free rotator GMF. The GMF is a Faraday rotator that has a square-shaped hysteresis loop and keeps constant Faraday rotation even when an external magnetic field in the opposite direction is applied. If the GMF is exposed to an external magnetic field in the opposite direction that is greater than coercive force  $H_c$ , the GMF is magnetized in opposite direction and Faraday rotation is reversed or the GMF is demagnetized completely. Note magnetic field that may be applied.

The coercive force of the chip-size GMF varies from about 400 to 2000 Oe individually. The coercive force depends on the external stress or the shape of a cross section in the cutting process. We measure coercive force  $H_c$  of each chip to see if the specification is satisfied before shipment. However, it should be noted that if the garnet is cut into a chip size, we do not guarantee the original coercive force.

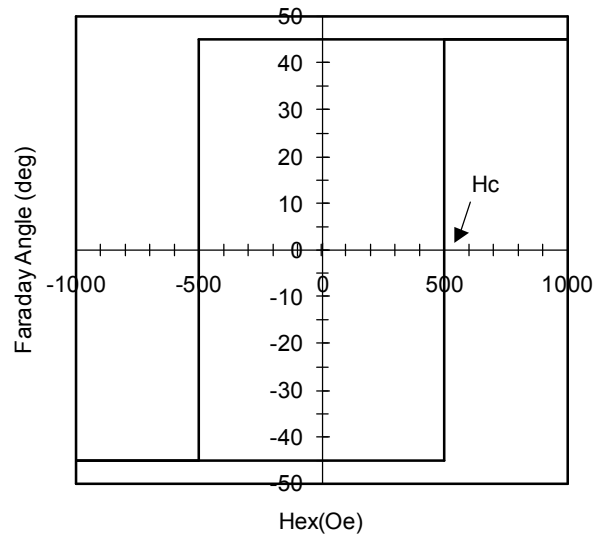


Fig. 6-6 Hex -  $\theta$  curve of GMF

Fig. 6-7 illustrates the temperature dependence of coercive force  $H_c$  of the GMF. The coercive force reduces as the temperature rises and loses its coercive force if the temperature becomes high for even a moment. Note that history of temperature applied to the GMF. Since applying mechanical stresses to the GMF also cause the coercive force to be lost, handle it with care.

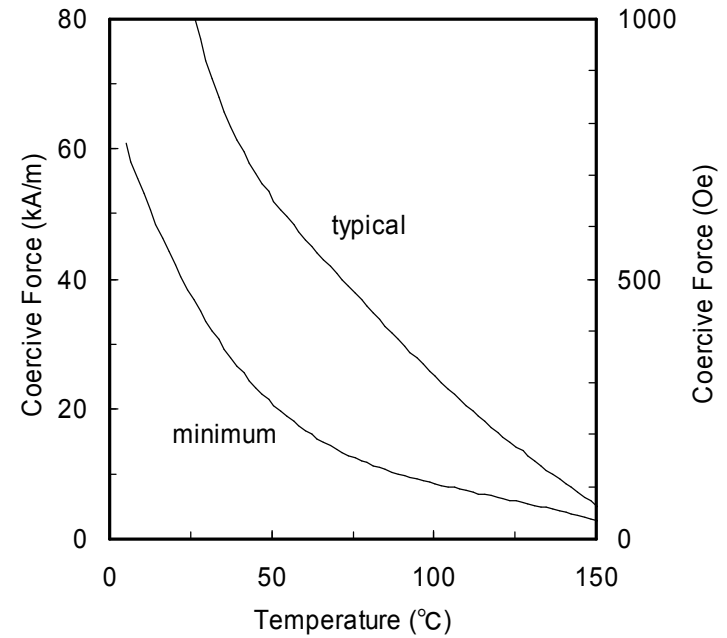


Fig. 6-7 Temperature dependence of  $H_c$  of GMF

### 6-3-2. How to use GMF

The GMF retains its magnetization and operates without an external magnetic field from a permanent magnet etc. However, the GMF is limited in the operating temperature when an external magnetic field applied. When the GMF is placed in an environment where the temperature is high and the magnetic field is strong, it is demagnetized and no longer functions as a Faraday rotator. Once the GMF has been demagnetized at high temperature, it no longer functions as a Faraday rotator even if it is cooled to room temperature.

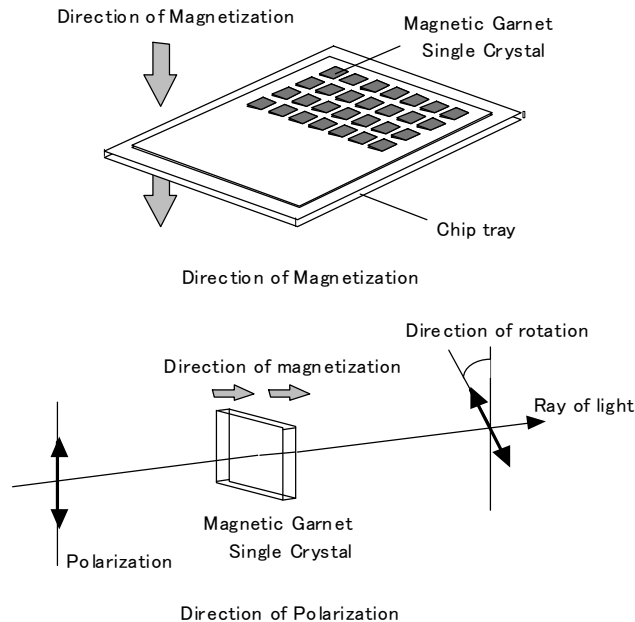


Fig.6-8 Direction of magnetization

The GMF is packed on a chip tray and magnetized before shipment. The magnetization oriented from the top side of the chip to the bottom side, as shown in Fig. 6-8. When light is incident on the chip in the direction of magnetization, the polarization plane rotators counterclockwise. Magnetization can also be performed by the user.

As previously described, the value of coercive force  $H_c$  varies from chip to chip. Fig. 6-7 illustrates the temperature dependence of  $H_c$  of the chip having a typical  $H_c$  and the lower limit of coercive force  $H_c$ . Coercive force  $H_c$  exhibits reversible changes with temperature. However, once the chip has been demagnetized at high temperature, the chip no longer exhibits the original coercive force and does not function as a Faraday rotator even if it is cooled to low temperature. In order to recover the coercive force, the chip must be magnetized again.

The GMF may be demagnetized to change its coercive force due to an external stress caused by a cutting operation etc.

The method of re-magnetizing the GMF will be described below. The GMF can be re-magnetized by applying a strong external magnetic field. An external magnetic field can be applied by an electromagnet or permanent magnet. If the GMF has been demagnetized for some reason, it need to be re-magnetized. To re-magnetized the GMF, it is recommended that an external magnetic field higher than 3000 Oe should be applied at a temperature of 40°C or higher. If the temperature is lower, it is necessary to apply a higher external field to recover the original coercive force. If the temperature is lower than room temperature (25°C), sufficient performance may not be obtained. The duration long enough to apply an external magnetic field is 1 second. If the user cuts the GMF, it is necessary to confirm that the individual chips have sufficient coercive force by, for example, applying a magnetic field of 400 Oe in the opposite direction and making sure that the individual chips are not magnetized in this direction.

#### 6-4. Magnetic compensation temperature and Curie temperature

RIG has peculiar temperatures called the magnetic compensation temperature ( $T_{comp}$ ) and Curie temperature ( $T_c$ ), at which the saturation field becomes zero. At a Curie temperature of  $220^{\circ}\text{C}$  to  $300^{\circ}\text{C}$  or higher, which depends on the product, the saturation magnetization and the Faraday rotation angle become zero. The magnetic compensation temperature, which also depends on the product, is lower than room temperature for all products. The saturation magnetization becomes zero at magnetic compensation temperature and the direction of magnetization is reversed before and after this temperature. When an external magnetic field is applied to RIG, the sign of the Faraday rotation angle is also reversed before and after the compensation temperature.

Fig. 6-9 shows an example of the Faraday rotation angle measured by applying an external magnetic field larger than its coercive force to our GMF. The magnetic compensation temperature of the GMF is about  $-10^{\circ}\text{C}$  at which the sign of the Faraday rotation angle is reversed. This is because the direction of saturation magnetization of RIG changes in accordance with the external magnetic field. For the GMF to which an external magnetic field is not applied, the sign of the Faraday rotation angle is not changed, as shown in Fig.6-10. It should be noted that an external magnetic field greater than its coercive force cannot be applied to the GMF.

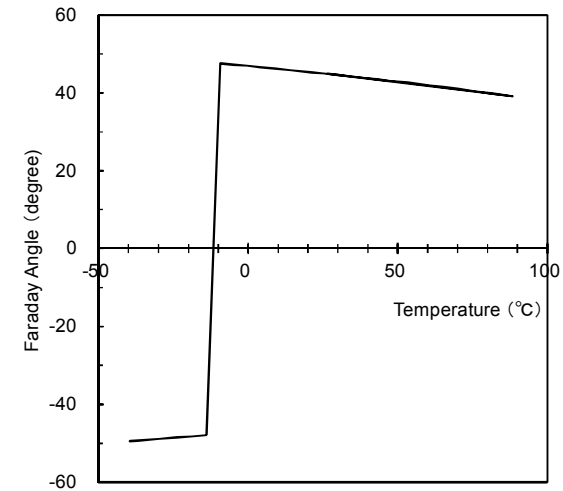


Fig. 6-9 Change in sign of Faraday rotation angle near compensation temperature with external magnetic field

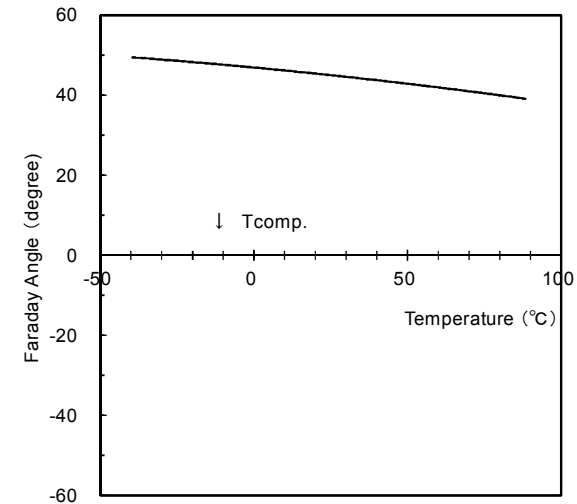


Fig. 6-10 Change in sign of Faraday rotation angle near compensation temperature without external magnetic field

## 7. Anti-Reflection Coating ( AR Coating )

### 7-1. AR coating types

Table.7-1. AR coating types

Item code	Index	Wavelength	Reflection (one side)
A	For air	Flexible	$\leq 0.2 \%$
E	For epoxy	Fixed , 1300 – 1650 nm	$\leq 0.2 \%$
N	No AR coating		
X	Else		

Table 7-1 lists the types of AR coatings that can be applied by GRANOPT. AR coatings are applied by the vacuum evaporation method. Coating A is an AR coating designed so that the reflection coefficient becomes small in the air at the specified center wavelength. Coating E is an AR coating designed to prevent reflection on a Faraday rotator in the state where the Faraday rotator is bonded to another optical component, and reduces the reflection coefficient to a small value over a wide range of wavelengths.

The types of AR coatings attached to both sides of Faraday rotator may be different each other. Please consult us for specific applications.

## 7-2. Features

### 7-2-1. Coating A

Coating A assumes air (refraction index  $n=1$ ) as a medium and has the minimum reflection coefficient at a specific wavelength. Coating A is made of  $\text{SiO}_2/\text{TiO}_2$  or  $\text{SiO}_2/\text{Ta}_2\text{O}_5$ . Fig. 7-1 shows a typical example of coating A of  $\text{SiO}_2/\text{Ta}_2\text{O}_5$  for 1550nm.

The GLB1064 consisting of the RIG ( $n=2.39$ , see Table 4-1) and the substrate ( $n=1.96$ ) can be coated with the coating A, but this coating cannot prevent the reflection caused by differences in the refractive indexes of the RIG and the substrate. In this case, it is recommended that the RIG should face the light source.

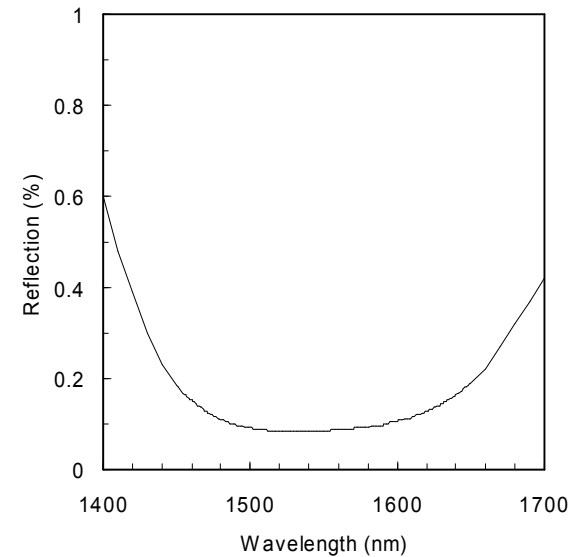


Fig. 7-1 Example of coating A (example of evaluation)

### 7-2-2. Coating E

Coating E is an AR coating designed to prevent reflection in the state where a Faraday rotator is bonded to another optical component, and reduces the reflection coefficient to a small value over a wide range of wavelengths from 1300nm to 1600nm. Coating E is made of SiO<sub>2</sub>/TiO<sub>2</sub>. Fig. 7-2 shows the result of simulating the performance of the AR coating when the refractive index of the adhesive changes.

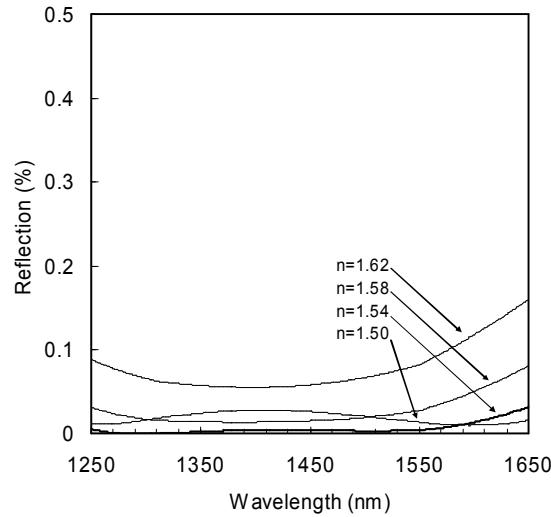


Fig.7-2 Calculation results

### 7-3. Incident angle

The performance of an AR coating degrades as the incident angle of light increases. Fig. 7-3 shows the calculation results of coating A.

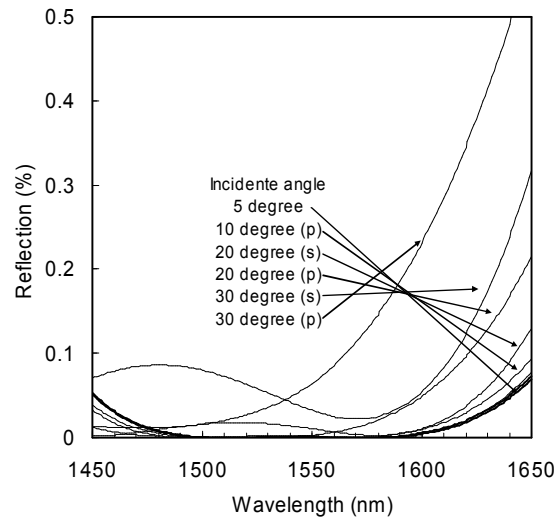


Fig.7-3 Calculation results

## 8. Reliability test

### 8-1. Environment test

Our products are tested under the following standard conditions. The items to be tested are the Faraday rotation angle, extinction ratio, insertion loss, surface quality, and adherence test of AR coatings. For the GMF, the coercive force is also evaluated.

High temperature storage test	100°C、2000hr
Low temperature storage test	-40°C、2000hr
Damp heat test	90°C、90%Rh、2000hr
Heat cycling test	-45°C – 90°C、1000cycles

## 8-2. Laser damage

### 8-2-1. Laser damage by plus laser

Fig. 8-1 illustrates damage caused by the following pulse laser.

From Fig. 8-1, we estimated that the minimum power that causes optical damage is about 100 MW/cm<sup>2</sup>.

Pulse laser	Beam diameter	18 μmφ
	Peak power	0-800 MW/cm <sup>2</sup>
	Pulse width	20 ns
	Pulse frequency	6 kHz
	Exposure time	2 sec

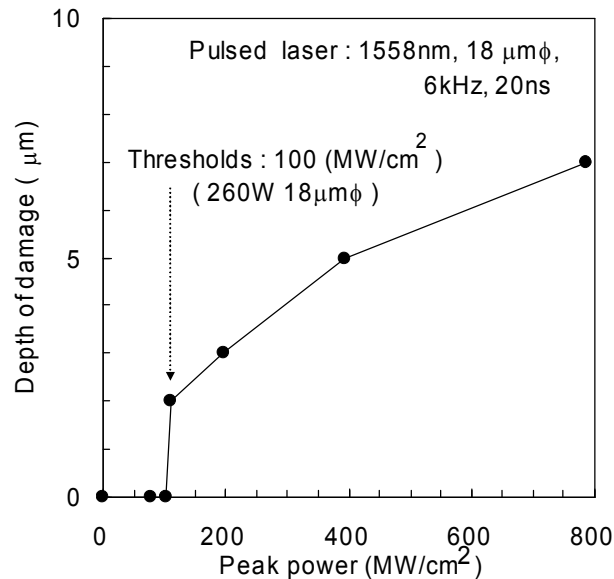


Fig. 8-1 Laser damage by pulse laser

### 8-2-2. Temperature rise by light absorption

Fig. 8-2 illustrates the relationship between the input power of light and the insertion loss. The Faraday rotator AiT1064 and a YAG laser with a wavelength of 1064nm and a beam diameter of 1mm are used for this measurement. The

A1T1064 has a insertion loss of about 0.8dB at a wavelength of 1064nm and an output power of 100mW or less. The marks ● represent the power of light pass through the A1T1064 from which the substrate has been removed. The marks ■ represent the transmittance. The power of transmitted light reduces significantly when to power or incident light is 200mW or more. This is because the temperature of RIG is raised by light absorbed by RIG and this increases the amount of light absorbed by RIG (refer to Section 5-1-4). This phenomenon occurs when temperature rise due to absorption of light is faster than the rate at which generated heat is dissipated. The marks ○ and □ represent the results of the same test when using the A1T1064 from which the substrate is not removed. Due to the heat sink effect of the substrate, generated heat is dissipated smoothly and an increase by absorption dose not reach 1W. At a wavelength from 1200 to 1600nm, it is expected that a temperature rise due to light absorption dose not occur until input power reaches several watts.

\* The A1T1064 has been discontinued. The GLB1064 is the substitute product.

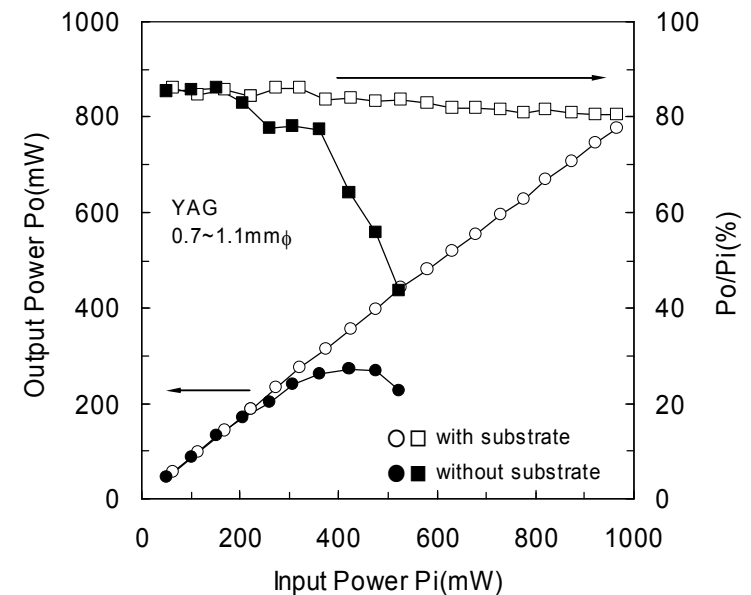


Fig. 8-2 Power of light and transmittance

## 9. Surface Quality

### 9-1. Standard specifications

Table. 9-1 11mm-square with AR coating

	Specification	Note
Aperture	An area of at least (product size - 0.5)mm square for the uncoated triangle(1x1mm)at each corner which is masked by a holding fixture when AR coated.	
Chipping	Absent in aperture	
RIG scratch	2 $\mu$ m $\leq$ Width $\leq$ 5 $\mu$ m 5 $\mu$ m $\leq$ Width	Total $\leq$ 10mm Absent
AR scratch	2 $\mu$ m $\leq$ Width $\leq$ 20 $\mu$ m 20 $\mu$ m $\leq$ Width	Total $\leq$ 10mm Absent
AR pinhole	50 $\mu$ m $\leq$ Width	Absent
Other defects	30 $\mu$ m $\leq$ Size $\leq$ 350 $\mu$ m 350 $\mu$ m $\leq$ Size	$\leq$ 5 pieces Absent

Table. 9-2 Chip size with AR coating

	Specification	Note
Aperture	Product size $\leq$ 1mm	$\leq$ (Product size - 0.2mm) $\phi$
	1mm < Product size < 2mm	$\leq$ (Product size) $\times$ 0.8 $\phi$
Chipping	Absent in aperture	
RIG scratch	Width < 2 $\mu$ m	No check
	2 $\mu$ m $\leq$ Width $\leq$ 5 $\mu$ m	(Product size) $\times$ 0.8
	5 $\mu$ m $\leq$ Width	Absent
AR scratch	Width < 2 $\mu$ m	No check
	2 $\mu$ m $\leq$ Width $\leq$ 20 $\mu$ m	(Product size) $\times$ 0.8
	20 $\mu$ m $\leq$ Width	Absent
AR pinhole	50 $\mu$ m $\leq$ Size	Absent
Other defects	Size < 10 $\mu$ m	No check
	10 $\mu$ m $\leq$ Size $\leq$ 30 $\mu$ m	$\leq$ 5 pieces
	30 $\mu$ m $\leq$ Size	Absent

### 9-2. Influence of defect and AR pinhole

Fig. 9-1 shows the results of calculation (solid line) and measurement (●) of the influence of a defect on insertion loss. The diameters of light beams are 300 $\mu$ m and 400 $\mu$ m and defect is assumed to be present at the center of the beam.

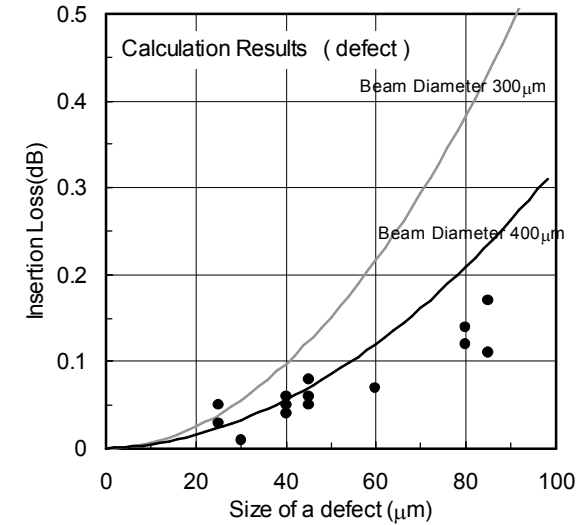


Fig. 9-1 Influence of defect

Fig. 9-2 shows the results of calculating the influence of an AR pinhole on insertion loss. Fig. 9-2 also shows the influence of an AR pinhole on the reflection coefficient. A defect and AR pinhole have an effect on the reflection coefficient and insertion loss to some extent, but the above calculations assume that a defect and pinhole are present at the center of the light beam. In reality, it can be seen from Fig. 9-3 that the probability of the presence of a defect or pinhole at the center of the light beam is small.

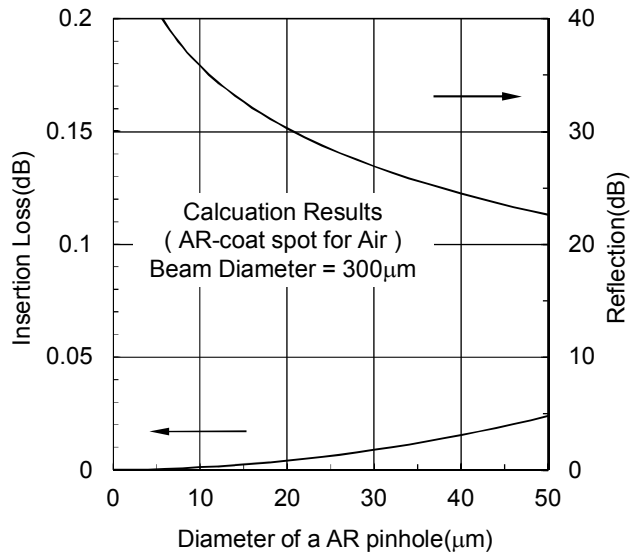


Fig. 9-2 Influence of AR pinhole

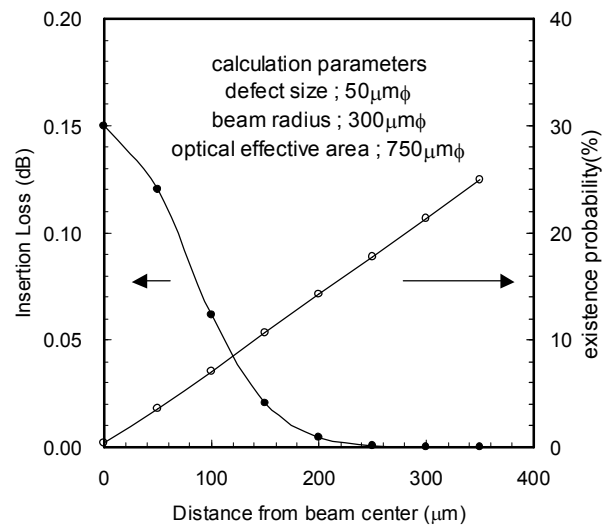


Fig. 9-3 Probability and influence of presence of defect and pinhole

### 9-3. RIG scratch and AR scratch

Fig. 9-4 shows the result of calculation and measurement (●) of the influence of a scratch. A light scratch on an AR coating does not affect insertion loss, so we provide separate specifications for these two scratches.

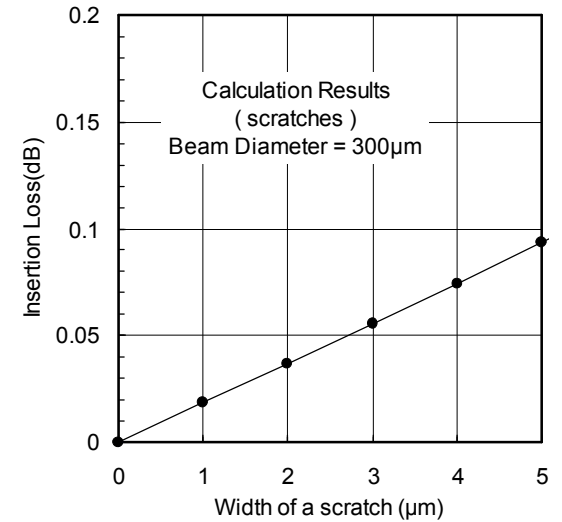


Fig. 9-4 Influence of RIG scratch on insertion loss

### 9-4. Chipping and corner break

GRANOPT defines chipping and corner break as shown in the figures below. Chipping is defined by the depth of deficit from the edge. Corner break is defined by the broken part. The standard specification defines that there is no chipping or corner break in the valid area.

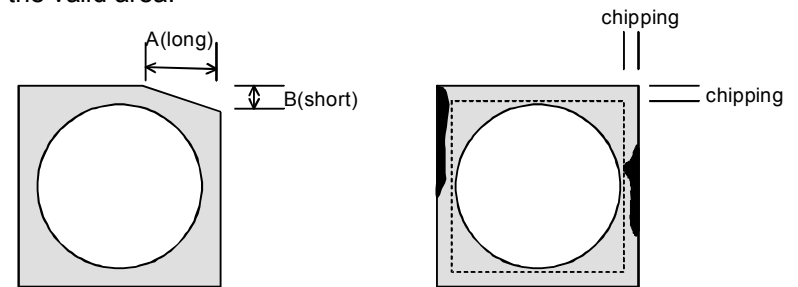


Fig. 9-5 Chipping and corner chip

## 10. Appendixes

### 10-1. Growth striation

The Photo 10-1 is an example of a growth striation that is observed with an infrared microscope. GRANOPT manufactures crystals of RIG by the LPE method, using the substrate GGG as a seed crystal. Since the temperature periodically changes and the crystal growth rate changes in the substrate GGG, the composition or the impurity density may change slightly, possibly causing annual ring-shaped lines. The striation of the substrate may be reflected on the RIG generated on the substrate GGG, and slight changes in the refraction index may be observed by an infrared microscope as shown in Photo 10-1.

We have scanned the entire surface to measure the Faraday rotation angle, extinction ratio, insertion loss, and other optical properties of RIG on which growth striation is generated and confirmed that the growth striation does not affect these optical properties.

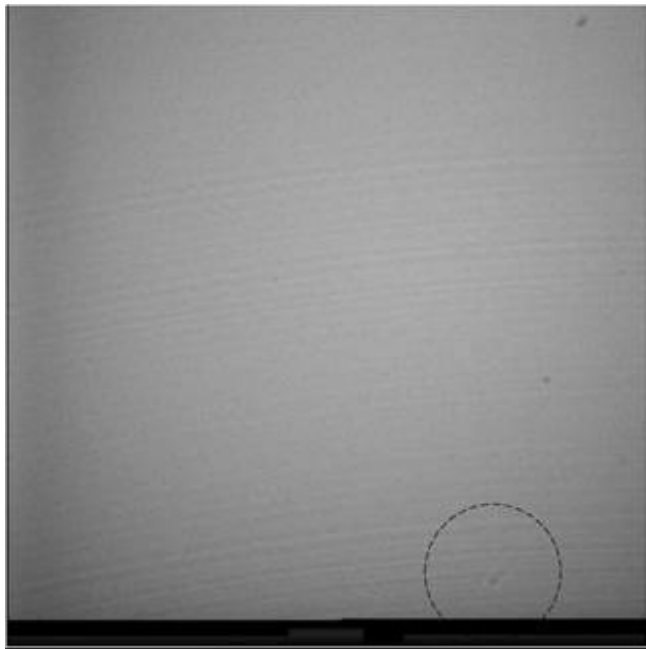


Photo 10-1 Growth striation and swirl

### 10-2. Swirl

The V-shaped line in Photo 10-1 called swirl which is generated on RIG manufactured by the LPE method. A swirl is a change in the refraction index that is originated from small defect generated in RIG and is observed by an infrared microscope. This change is caused by a slight change in the composition under influence of convection in crystal growth process. We have also confirmed that the swirl does not affect the optical properties.

### 10-3. Surface undulation

There is a nano-scale undulation on the surface of RIG. Fig. 10-1 exaggeratedly shows effects of an undulation on reflected light. We suppose that stripes rarely observed by a metallurgical microscope are formed when this undulation has an effect on reflected light in the visible band, which falls outside the scope of design of AR coating.

In a crystal growth process, RIG has inner stress caused by differences the thermal expansion coefficient between RIG and the substrate. If the substrate GGG is removed, the individual products suffer warping due to this inner stress. We polish the while relaxing this warping and finish it in CMP. We suppose that the surface undulation is caused by this etching of CMP.

As a result of evaluation of the effect of the undulation on optical properties, we have confirmed that the surface undulation does not have a great effect because the surface undulation is significantly smaller than the wavelength of light.



Photo 10-2 Surface undulation

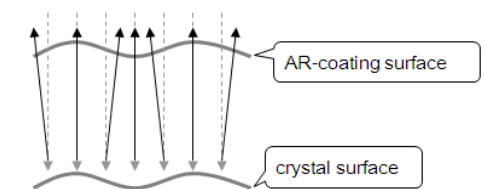


Fig. 10-1 Observation principle